Solution-Grown Silicon Nanowires for Lithium-Ion Battery Anodes

Candace K. Chan,[†] Reken N. Patel,[‡] Michael J. O'Connell,[§] Brian A. Korgel,[‡] and Yi Cui[⊥,*]

[†]Department of Chemistry, Stanford University, Stanford, California 94305, [‡]Department of Chemical Engineering, University of Texas at Austin, Austin, Texas 78712, [§]Sp2 Carbon, 523 Dougherty, Morgan Hill, California 95037, and [⊥]Department of Materials Science and Engineering, Stanford University, Stanford, California 94305

ABSTRACT Composite electrodes composed of silicon nanowires synthesized using the supercritical fluid—liquid—solid (SFLS) method mixed with amorphous carbon or carbon nanotubes were evaluated as Li-ion battery anodes. Carbon coating of the silicon nanowires using the pyrolysis of sugar was found to be crucial for making good electronic contact to the material. Using multiwalled carbon nanotubes as the conducting additive was found to be more effective for obtaining good cycling behavior than using amorphous carbon. Reversible capacities of 1500 mAh/g were observed for 30 cycles.

KEYWORDS: silicon nanowires · carbon nanotubes · lithium-ion battery anodes

There has been increasing interest in using nanomaterials for advanced lithium-ion battery electrodes, particularly for increasing the energy density by using high specific capacity materials. An attractive alternative material for the graphite anode is silicon, largely due to its wide abundance and order of magnitude higher charge storage capacity (theoretical values of 4200 *vs* 372 mAh/g for graphite). However, the insertion of lithium into silicon to form the fully lithiated $Li_{4.4}Si$ stoichiometry is associated with a large volume change of >300%, which can cause the material to pulverize and lose contact with the current collector, resulting in a decrease in charge storage capacity over time.[1] The use of nanostructured silicon films[2−9] has led to improvements in both capacities and cycle life, due to facile accommodation of the volume change and strain relaxation. Our recent work[10] showed that high capacities (>3500 mAh/g) could be achieved with an electrode architecture consisting of silicon nanowires (SiNWs) grown vertically off of a metallic current collector using the vapor−liquid−solid (VLS)[11,12] method. With this architecture, each SiNW was adhered to the substrate and additional conducting additive or binder was not required. The good electrochemical performance is attributed to the small size of the nanowires allowing for efficient volume change without pulverization, good electronic contact between each nanowire and the substrate, and good electron transport along the length of each nanowire. The development of a variety of Si core−shell NWs and nanotubes has provided interesting materials for further development.[13−16] For VLS-grown nanowires, one important question is how to integrate them into traditional battery electrode coating processes, where the active material is mixed with a conducting additive and binder, suspended into a slurry, and coated onto a current collector as a composite. These processes are used on a large scale commercially. Given that lowering the price of batteries is a major goal, the cost of the processing and fabrication of the electrode must be taken into account when considering the use of any new material as a battery electrode.

Therefore, we have attempted to make a silicon nanowire-based electrode using the traditional slurry method. Although the scaled synthesis of VLS NWs is possible in the future, the VLS method for growing SiNWs thus far is limited in that it is difficult to synthesize large quantities of nanowire material on the substrate (only ~200−250 μg/cm^2 or ~0.75 mg/h), and furthermore, the SiNWs must be released from the substrate using techniques such as ultrasonication and can be easily broken in the process. Solution-based analogues of the VLS method have been developed by Korgel's group,[17−20] and the large-scale synthesis of SiNWs (>45 mg/h) has been demonstrated using the supercritical fluid−liquid−solid (SFLS) growth technique. Our goals here are two-fold: (1) to evaluate a SiNW electrode made using the

*Address correspondence to yicui@stanford.edu.

Received for review October 13, 2009 and accepted February 19, 2010.

Published online March 4, 2010.
10.1021/nn901409q

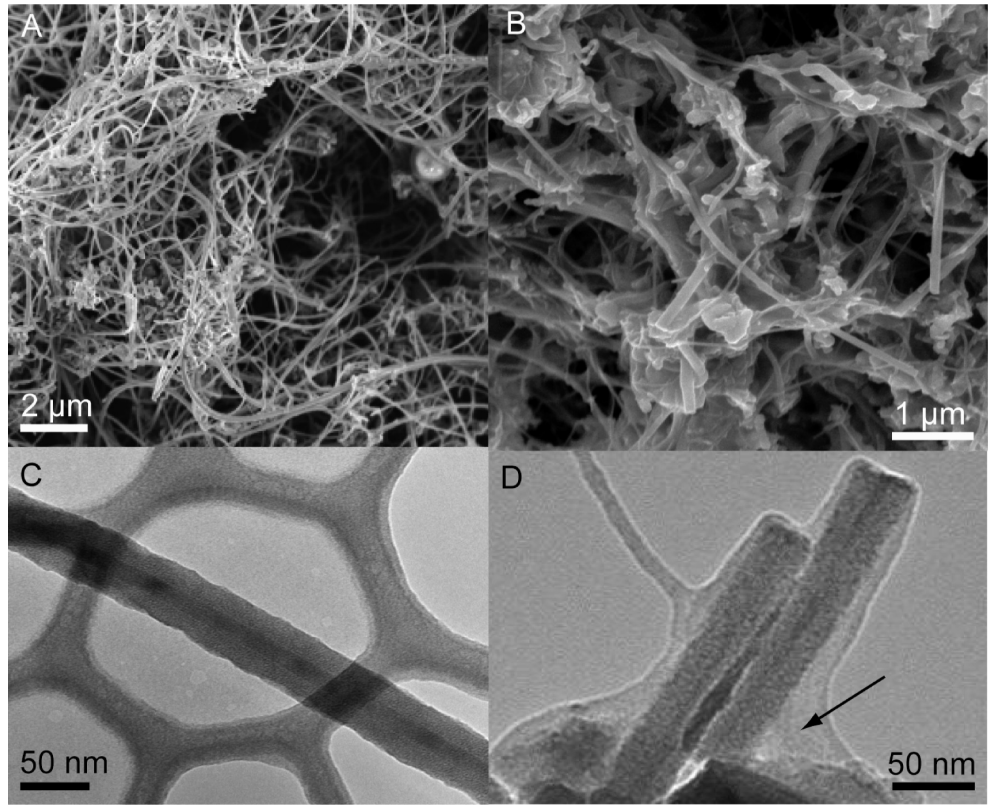

Figure 1. SEM image of SFLS SiNWs (A) as-grown, (B) after carbon coating. TEM image of SFLS SiNWs (C) as-grown, (D) after carbon coating, with arrow indicating carbon.

traditional slurry method, and (2) to compare the VLS SiNW electrode architecture with the composite electrode made using the slurry method to understand the role of electrode design in electrochemical performance.

RESULTS AND DISCUSSION

A typical scanning electron microscopy (SEM) image of the SFLS SiNWs is shown in Figure 1A. While the majority of the synthesized product consist of SiNWs with an average diameter of 24.6 ± 12.0 nm and a length of >10 μm, there were also some irregular and spherical particles present, which were 2.5 ± 1.0 μm in size. The as-grown SiNWs were single crystalline but often had a thin coating (6.9 ± 3.4 nm), as shown in the transmission electron microscopy (TEM) image in Figure 1C. This shell is composed of polyphenylsilanes that form as a reaction byproduct during the large-scale SFLS growth of SiNWs (>10 mg).[15] Carbon coating[21] of battery materials has been frequently used to improve the electron flux to the surface of the Li insertion material, aid electron transport between particles, and to improve rate performance. For Si, carbon coating may also be used to buffer the large volume changes and control the solid electrolyte interphase (SEI) formation, as well as improve the electronic conductivity of the electrode. Carbon coatings based on chemical vapor deposition[22] or high-energy milling with polymers[23] may form SiC on the surface of the Si, which is electrochemically inert to lithium.[22] Thus, the SiC plays no role other than to add extra unwanted weight, although some reports have claimed improved contact/conductivity at the interface between Si and carbon.[24] High-energy ball milling will also likely destroy the nanowire morphology. For these reasons, carbon coating was performed using the carbonization of an organic precursor, in our case, sucrose, which is known to form amorphous carbon without any SiC phases.[25−28] Figure 1B,D shows an SEM and TEM image, respectively, of the SiNWs after carbon coating. From these images, it is clear that the morphology and crystallinity of the SiNWs is preserved after the carbonization process. It appears that the carbon coating is not conformal around all of the SiNWs; rather, pairs or bundles of SiNWs may be coated, as shown in Figure 1D. This is likely due to inadequate mixing and penetration of the sucrose molecules into the SiNW bundles prior to pyrolysis. This may lead to the discrepancy observed in the mass of carbon coating after the pyrolysis for different samples.

Thermogravimetric analysis (TGA) of sucrose using the same pyrolysis conditions yielded a weight loss of 80% (Supporting Information, Figure S1A). However, when using the pyrolysis for carbon coating of the SiNWs, weight losses corresponding to 72−98% of the mass of sucrose were observed for different SiNW samples, calculated based on the mass of the SiNWs be-

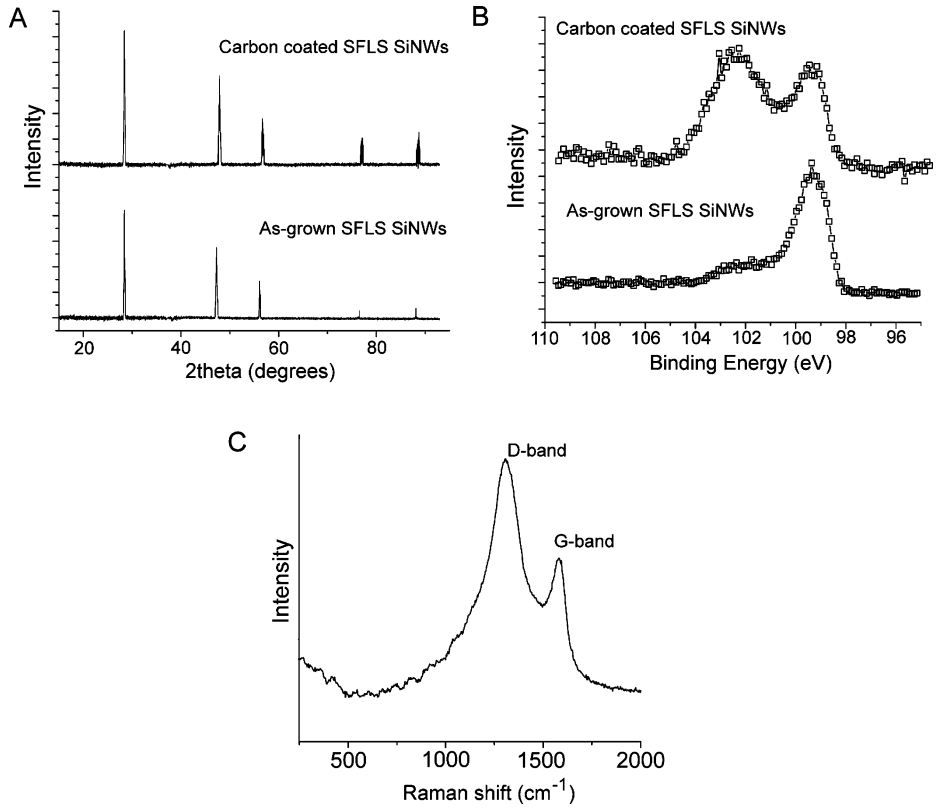

Figure 2. (A) XRD pattern of as-grown and carbon-coated SFLS SiNWs. (B) High-resolution Si 2p scan of as-grown and carbon-coated SLFS SiNWs. (C) Raman spectrum of pyrolyzed sugar.

fore and after coating and using the initial mass of sucrose. It is also possible that some of this weight loss was due to removal of residual organic species from the surface of the SiNWs. The SFLS synthesis is carried out in an organic solvent, and there may have been residual organic material that had not been completely removed during postsynthesis purification. To investigate this, TGA was performed on pristine SFLS SiNWs, without mixing with sucrose. This was to see how clean the surfaces of the SiNWs were after the postsynthesis cleaning steps. As shown in Figure S1B, there was a ~6% weight loss, indicating that there was indeed some residual contamination on the SiNWs that was removed during the heating ramp to 700 °C. Mass spectrometry (Figure S1C) identified the major removed species as water and either nitrogen or carbon monoxide (they have the same mass and cannot be distinguished here). Benzene, oxygen, and water were also observed. The origin of the benzene may be from the decomposition products of the polymeric phenylsilane coating on the nanowires. The rest of the species can be explained as adsorbed species and/or oxidation products of organic contaminants. These results confirmed that the SFLS SiNWs were coated with a thin organic layer that was not removed after the synthesis.

X-ray diffraction (XRD) of the SiNWs as-grown and after carbon coating (Figure 2A) showed only reflections due to Si. This confirmed that not only were the crystalline cores of the SiNWs preserved, but there was no SiC formation during the pyrolysis. There were also no reflections detected for the carbon coating, indicating that it is amorphous. This observation is consistent with other studies using this coating method.[21]

Raman spectroscopy of the pyrolyzed sugar (Figure 2C) displayed features corresponding to the G band (found in carbons with high degrees of order) at 1581 cm^{-1} and the D band (found in disordered carbons) at 1302 cm^{-1}. The ratio of the peak intensities, I_D/I_G, can be used to asses the crystallinity of the carbon. Here I_D/I_G was 5.24, indicating the carbon coating was highly disordered, that is, amorphous. This is consistent with the XRD results.

X-ray photoelectron spectroscopy (XPS) was used to investigate the local structure and bonding of the SiNW surface. The XPS data for the as-grown SiNWs and coated SiNWs are shown in Figure 2B. The Si 2p spectrum for the as-grown SiNWs shows a peak at 99.3 eV corresponding to zero-valent silicon. In contrast with VLS-grown silicon nanowires, which show a second peak in the Si 2p region at 103.12 eV due to native oxide formation,[29] SFLS-grown silicon nanowires do not, due to the polyphenylsilane coating. Instead, a shoulder is observed from ~100 to 103 eV, which represents the Si−C and siloxane species contained within the polymer coating. After the carbon coating, the high-energy peak increased in intensity, indicating that the

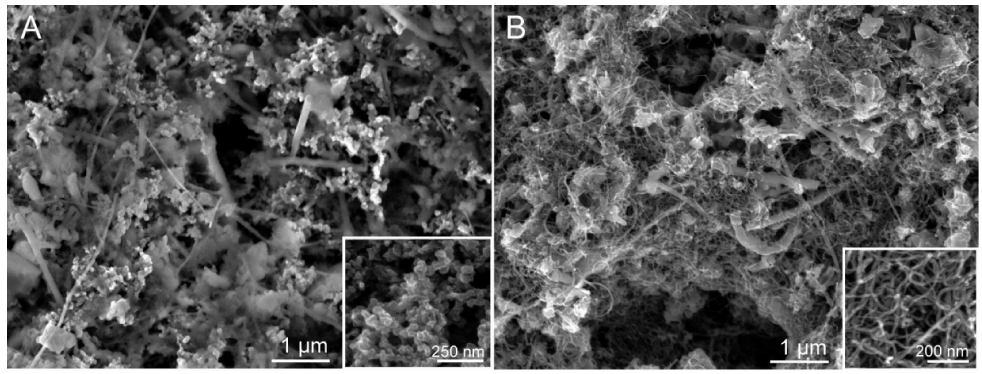

Figure 3. SEM images of SiNW composite electrodes prepared with 78 wt % SiNWs, 12 wt % CMC binder, and 10 wt % conducting carbon comprising of (A) carbon black, or (B) multiwalled carbon nanotubes. Insets show each type of carbon only.

SiNWs were coated with a film. The C 1s peak looked very similar before and after the carbon coating, but the O 1s peak showed a shift to higher energies after the coating, suggesting that C═O bonds[30] may have been formed (Figure S2, Supporting Information).

Different slurry compositions were made for galvanostatic cycling using either carbon black (CB) or multiwalled carbon nanotubes (MWNTs) as the conducting additive. The SiNWs were mixed with CB and binder (carboxymethyl cellulose, CMC) at a weight ratio of 78:12:10. An SEM image of the electrode is shown in Figure 3A, with the inset image showing the CB particles alone. Because the size of the carbon particles is on the same order as the size of the SiNWs, the CB does not form a percolating network with the SiNWs. Rather, the particles only make contact with some of the nanowires. Figure 3B shows an electrode made using the same ratio of materials except with MWNTs instead of CB. Although carbon nanotubes (CNTs) have been studied as active materials,[31−34] large irreversible capacity loss in the first cycle due to SEI formation, a large hysteresis between charge and discharge voltages, and insufficient long-term cyclability made CNTs unsuitable replacements for graphite. However, CNTs have been used to replace CB as the conducting additive and have been found to lead to improvements in capacity and cycle life in different anode[35,36] and cathode[37−39] systems. There have been several reports[40−43] of the growth of carbon nanotubes on the surface of Si particles. However, this can lead to SiC formation. To avoid this, we used simple mixing (with magnetic stirring) of commercially available MWNTs with our SiNW slurry. As shown in Figure 3B, this mixing was adequate to make a film with good contacts between the MWNTs and the SiNWs. For small diameter SiNWs, there can be multiple points of contact with the MWNTs, with the MWNTs often completely wrapping around the SiNW. This may help to ensure good connectivity throughout the composite. However, for larger diameter SiNWs and particles, this may not be possible. Also, the MWNTs formed a good network with the SiNWs and other MWNTs, ensuring good transport of electrons throughout the electrode.

The electrochemical potential spectroscopy (EPS) measurement (Figure 4A) shows the presence of amorphous Si, which may be present as a crystalline-amorphous core−shell structure in the SiNWs, as observed in the TEM (Figure 1C), or as the micrometer-sized particles observed in the SEM (Figure 1A). Our previous EPS studies[44,45] on VLS SiNWs found that lithiation of the crystalline SiNW occurs at 0.125 V *vs* Li/Li^+, whereas lithiation of amorphous Si occurs at higher potentials (~0.22 V *vs* Li/Li^+). During the first lithiation step, a small peak at about 0.6 V is observed from initiation of the SEI formation[29] due to the reduction of the electrolyte. The lithiation peak of amorphous Si is seen (indicated by an arrow) as well as the lithiation of crystalline Si. At the end of the first lithiation, all of the material has been transformed into amorphous Li_xSi. In the second cycle and subsequent cycles (not shown), the electrochemical lithiation of the SFLS SiNWs follows the same structural transformations as observed in the VLS SiNWs.[44]

The galvanostatic cycling data of the SFLS SiNW electrodes are shown in Figure 4B. The first charge capacity has been omitted for clarity, but the charge and discharge capacities for first three cycles are shown in the inset. When analyzing galvanostatic cycling data, it is important to take note of the difference between the charge (lithiation) and discharge (delithiation) capacities, as this is an indication of reversibility (Coulombic efficiency). The discharge capacities are also important because this represents how much charge is available to supply to a cathode in a full cell. The uncoated sample consisted of pristine SiNWs mixed with carbon black and CMC at a weight ratio of 78:12:10. This electrode performed poorly, with an irreversible capacity loss of 66% in the first cycle and rapid capacity loss from an initial discharge capacity of 1077 mAh/g fading to 151 mAh/g after 75 cycles. The low discharge capacities suggest that a large amount of the Si is not actively participating in the electrochemical reactions due to being out of electronic contact with the current collec-

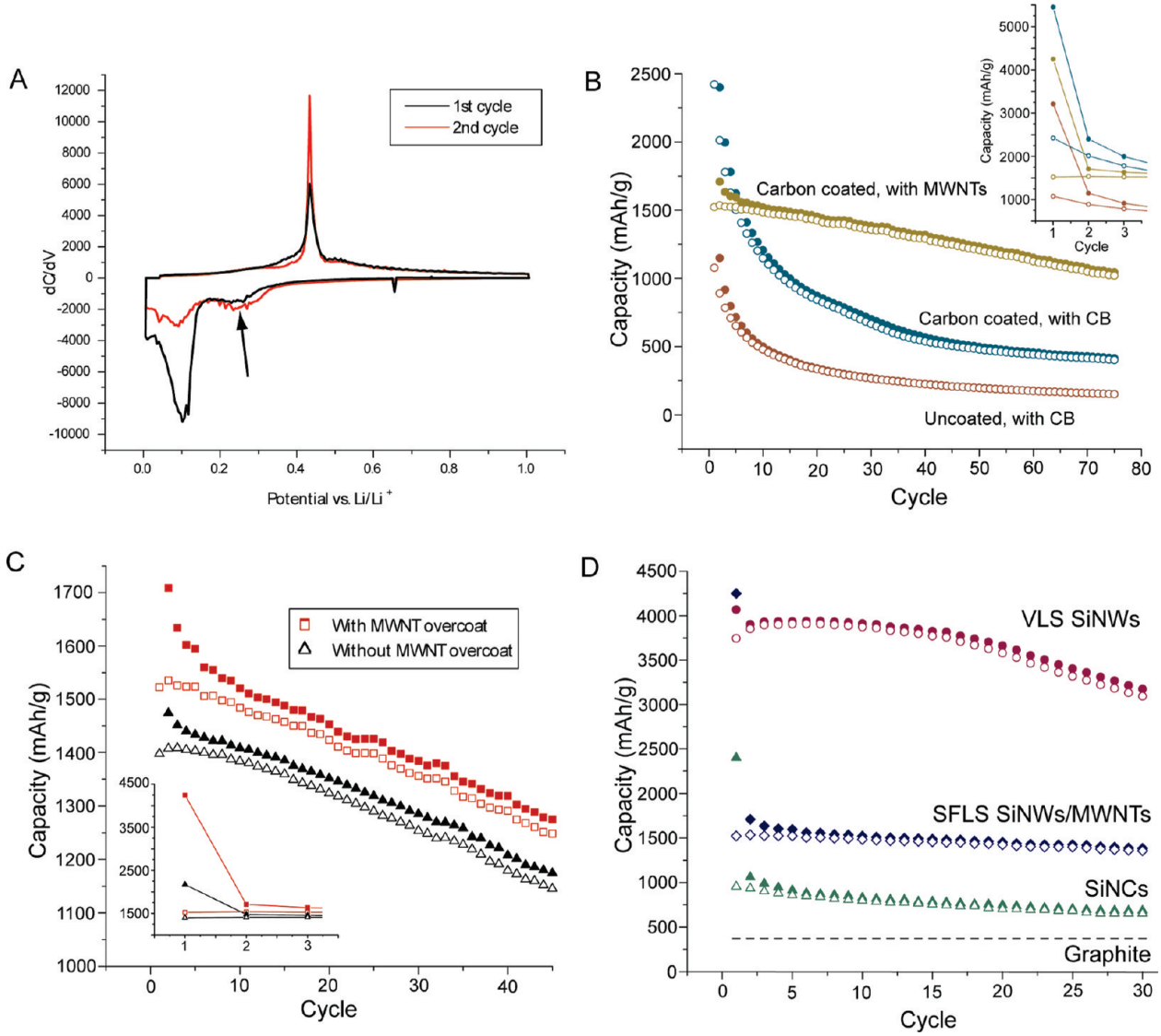

Figure 4. (A) Electrochemical spectroscopy data for the first two cycles of the reaction of Li with the SFLS SiNWs. The arrow indicates the lithiation of amorphous Si, confirming the presence of amorphous Si in the sample, either as a shell on the SiNWs or in the form of micrometer-sized particles. (B) Capacity *vs* cycling data for SFLS SiNWs uncoated and mixed with carbon black, carbon-coated and mixed with carbon black, and carbon-coated and mixed with multiwalled carbon nanotubes with an additional nanotube overcoat layer. The first cycle is omitted for clarity but is shown in the inset. (C) Capacity *vs* cycling data for SFLS SiNWs mixed with multiwalled carbon nanotubes with and without an additional nanotube overcoat layer. The first cycle is omitted for clarity but is shown in the inset. (D) Comparison of the cycling performance for a SiNW electrode grown using the vapor−liquid−solid method on a metallic current collector, the SFLS SiNW/MWNT mixture with MWNT overcoat, Si nanocrystals, and the theoretical capacity for graphite.

tor. The large irreversible capacity loss may also be due to NWs losing electronic contact after the initial volume change. The carbon-coated SiNW sample mixed with carbon black and CMC at a weight ratio of 65:9:8 (with the carbon coating accounting for 18 wt %) also displayed a high irreversible capacity loss of 55% and fast degradation, although the capacities achieved were higher than without the carbon coating. This illustrates the importance of the coating for improving electronic conductivity in the electrode. With the coating, a high initial charge capacity of 5450 mAh/g was observed in the first cycle. As the theoretical capacity for the full lithiation of Si is only 4200 mAh/g, all of the excess capacity is likely due to SEI formation on the additional carbon from the coating. A sample containing carbon-coated SiNWs mixed with MWNTs and CMC at a weight ratio of 78:12:8.5 (with the carbon coating accounting for 1.5 wt %) was found to display even higher capacities than the electrodes made with CB as the conducting agent, although still much lower than the theoretical capacity. This may be due to improved electronic conductivity of the MWNT network compared to the CB, which has been previously observed.[46] Also, the MWNTs may improve the resiliency of the electrode and help to buffer the large volume changes.[41,47] Control tests on electrodes made from MWNTs and CMC only (Figure S3, Supporting Information) showed stable reversible capacities of about 110 mAh/g, which is due to capaci-

tance stored in the electrochemical double layer. This extra charge does not account for all of the improvement in the specific capacities observed in the SiNW/MWNT sample. Rather, the MWNTs allow more electron flux to reach the SiNWs, allowing more of the active material to participate in the electrochemical reactions.

To understand the effect of the MWNTs, an additional layer of MWNTs was applied to the top of an electrode with the same composition. The purpose of this overcoat layer was to completely cover all of the SiNWs and ensure that all of the active material is electrically connected. An intentionally thick layer was used, resulting in the overcoat making up 70 wt % of the total electrode mass, with the SiNWs making up only 24 wt %. The cycling results for this sample are shown in Figure 4C (labeled as "with MWNT overcoat") compared to the results for a sample without the overcoat (78% SiNWs, 12% MWNTs). The first charge capacity and irreversible capacity loss were much higher in the sample with the overcoat than without it (4250 *vs* 2171 mAh/g). This is likely due to additional SEI formation on the MWNTs as seen by the plateau in the voltage curve (Figure S4) at around 0.6 V, the potential at which SEI formation occurs on carbon (Supporting Information). The discharge capacities in the first cycle were very close for both samples, indicating that the MWNT overcoat did not significantly improve electronic conductivity. Indeed, long-term cycling showed a similar degradation rate for both samples (Figure 4C), although the sample with the overcoat had higher capacities by about 7−8%.

In Figure 4D, the capacities for the sample with the MWNT overcoat are compared with capacities observed for SiNWs grown on a metallic substrate using the VLS method, a film of SiNCs (from ref 4), and the theoretical capacity for graphite. The SFLS SiNWs have higher capacities than the SiNCs, which is likely due to improved particle−particle interactions between the SiNWs and the MWNTs as well as other SiNWs. Although the SiNCs can also undergo the large volume change upon Li insertion, the particles can easily impinge on each other and become displaced from the electrode. The 1D nanowire shape is helpful for making a network to keep all of the active material attached to the substrate. However, the capacity of the SFLS SiNW electrode is much lower than expected, based both on the theoretical capacity for $Li_{4.4}Si$ (4200 mAh/g) as well as the experimentally achieved capacities for the VLS SiNWs. Even with a vast excess of conducting additive in the form of the MWNT overcoat, the achieved capacities did not improve too much. There may be several reasons for this. First, the quality of the SFLS SiNWs may not be equal to that of the VLS SiNWs. The surface of VLS SiNWs has been well-characterized as a clean surface covered only with a native SiO_2 layer 1−3 nm thick. In contrast, the SFLS SiNWs have a polymeric phenylsilane coating on the surface of the wires as a result of the synthesis, as suggested by XPS and TEM data. These compounds may act as a barrier to Li-ion insertion into the Si. Future work on cleaning and using various surface modifications may shed more light on this matter. Second, there appear to be significantly more non-nanowire particulates in the SFLS SiNW sample than with the VLS SiNW sample. Although non-nanowire particulates can also occur in the VLS growth, they can be avoided by tuning the growth conditions such that almost none can be found. On the other hand, micrometer-sized amorphous Si particles are a common byproduct of the SFLS SiNW synthesis. These micrometer-sized particles will contribute to the weight of the electrode without displaying good electrochemical performance, lowering the performance for the ensemble as a whole. Fine tuning the synthesis or using postsynthetic separation techniques to acquire a purified nanowire sample will be beneficial in further understanding this matter. Third, the VLS electrode design may be more effective for transporting charge from the current collector to the SiNWs. This is because the NWs are grown directly on a metallic substrate and do not have to rely on binder and carbon to be electronically connected. Because Si undergoes large volume changes during lithiation/delithiation, the mechanical properties of the binder and nanotubes may not be sufficient enough to buffer the volume changes and maintain electrical connection. However, because the large excess of carbon supplied as the MWNT overcoat was not found to significantly improve the capacity, and because the degradation rate of the VLS NWs was actually higher than that for the SFLS NWs, it is still unclear what role the electrode design plays. Capacities of 2800 mAh/g have been obtained from an electrode composed of porous Si nanoparticles mixed with carbon black prepared and coated from a slurry very similar to the method we used.[7] While these capacities are higher than the SFLS SiNW electrodes evaluated here, they are still lower than the VLS SiNW electrodes. More studies will be needed to understand the relationship between the electrode design and electrochemical performance.

Nonetheless, our SFLS SiNW/MWNT composite electrode still displays better performance than other reports in the literature that used ball milling of Si and CNTs or direct CVD growth of CNTs onto Si. These techniques are energy intensive and require many steps. Our procedure shows that better performance can be achieved using simple mixing. We attribute this improvement to the good conductivity and connectivity of the network made from the SiNWs and MWNTs. Future work will focus on improving the capacities and cycle life through optimization of synthesis, surface treatments to reduce side reactions and irreversible capacity losses, and evaluation of rate performance and different mass loadings.

METHODS

SiNWs were synthesized by gold-seeded SFLS growth in toluene, as previously described by Tuan *et al.*[20] Dodecanethiol-coated Au nanocrystals with 2 nm diameters were used as seeds at a reaction temperature and pressure of 490 °C and 10.3 MPa, respectively. The phenylsilane concentration was 70 mM, and the Si/Au ratio was 700. After the reaction, the nanowires were collected from the walls of the reactor and purified by dispersing in 10 mL of chloroform and 5 mL of ethanol, followed by centrifugation at 8000 rpm for 5 min. The precipitated SiNWs were collected and purified by this process of redispersion and precipitation two more times. A typical reaction yields ~30 mg of SiNWs. The SiNWs were characterized using transmission electron microscopy (TEM, Tecnai G2 Spirit BioTWIN), scanning electron microscopy (SEM, FEI XL30 Sirion), X-ray photoelectron spectroscopy (PHI 5000 VersaProbe, Al Kα X-ray source), X-ray diffraction (PANalytical X'Pert, Cu Kα radiation), and thermogravimetric analysis (TGA, Netzsch STA 449 F3 Jupiter coupled with mass spectrometer QMS 403C). The effect of a carbon coating on the SiNWs was also evaluated. The SiNWs were coated with carbon using a technique[21] previously used to coat battery materials: mixing with sucrose and pyrolyzing in forming gas (2% H_2 in Ar) at 700 °C for 1 h. To avoid introducing damage to the SiNWs from mechanical grinding, the sucrose was dissolved in a minimum amount of water and added to the boat containing the SiNW powder.

The composite electrodes were made by mixing the SiNWs with sodium carboxymethylcellulose (CMC) (MW 90 000, Aldrich) binder and commercially available conducting carbon additive in water. All masses were measured using a microbalance with 0.1 μg resolution (Sartorius SE2). All calculated capacities are based on the weight of the active Si material only. CMC was the binder of choice in this study because it has been previously found to be a superior binder for silicon electrodes compared to other polymers.[48,49] The carbon used was either SuperP Li conducting carbon black (Timcal) or multiwalled carbon nanotubes (CNano). The carbon black (CB) was used as received, but the multiwalled carbon nanotubes (MWNTs) were rather hydrophobic and had to undergo surface oxidation treatments to aid suspension in water. Briefly, the MWNTs were digested in nitric acid at 70 °C, then filtered and washed with water and KOH, and afterward heated in a vacuum oven at 120 °C until dry. The slurry was coated onto Cu foil using a motorized drawdown machine with a Mayer rod applicator. The mass loading was similar to that used in our previous studies using VLS SiNWs, ~200 μg/cm^2 of Si. We note that higher mass loadings can be easily obtained using the slurry coating method, but we wanted to compare the role of different electrode architectures on the electrochemical performance for similar amounts of active material. The electrodes were dried at 100 °C in air and then 200 °C in Ar just prior to cell assembling to remove any residual water. Half-cells were fabricated out of the SiNW electrode, Li metal foil, and Celgard 3401 separator soaked in electrolyte. The electrolyte was 1.0 M $LiPF_6$ in 1:1 w/w ethylene carbonate/diethyl carbonate (Novolyte). The cells were assembled inside an Ar-filled glovebox and sealed in aluminized polyethylene laminate bags.

The electrochemical performance of the SiNWs was evaluated using electrochemical potential spectroscopy (EPS)[50] and galvanostatic cycling. For EPS, the potential of the SiNW electrode was stepped between the open circuit voltage (around 2.5 V *vs* Li/Li^+) and the lower cut off voltage (0.01 V *vs* Li/Li^+) using 5 mV increments. The current was measured in each step until the value was higher than the threshold corresponding to the current of the C/20 charge rate (20 h to charge based on the theoretical capacity of 4200 mAh/g). Each step was then integrated to get the differential capacity. EPS measurements were made using a Biologic VMP3, and galvanostatic measurements were made using a Maccor 4300 with cycling between 1.0 and 0.01 V *vs* Li/Li^+ using a C/5 rate.

Acknowledgment. The authors thank Z. Chen for assistance with the Raman spectroscopy measurements, and F. La Mantia for assistance with the TGA measurements. C.K.C. acknowledges support from the National Science Foundation and Stanford Graduate Fellowships. Y.C. acknowledges support from the King Abdullah University of Science and Technology (KAUST) Investigator Award (No. KUS-I1-001-12). R.N.P. and B.A.K. acknowledge funding from a DOE Energy Frontier Research Center Award (DE-SC-001091).

Supporting Information Available: Experimental details for SFLS SiNW synthesis, thermogravimetric analysis of sucrose, X-ray photoelectron spectroscopy data, galvanostatic cycling of MWNT control samples, voltage profile of SiNW/MWNT samples. This material is available free of charge *via* the Internet at http://pubs.acs.org.

REFERENCES AND NOTES

1. Boukamp, B. A.; Lesh, G. C.; Huggins, R. A. All-Solid Lithium Electrodes with Mixed-Conductor Matrix. *J. Electrochem. Soc.* **1981**, *128*, 725–729.
2. Gao, B.; Sinha, S.; Fleming, L.; Zhou, O. Alloy Formation in Nanostructured Silicon. *Adv. Mater.* **2001**, *13*, 816–819.
3. Green, M.; Fielder, E.; Scrosati, B.; Wachtler, M.; Moreno, J. S. Structured Silicon Anodes for Lithium Battery Applications. *Electrochem. Solid-State Lett.* **2003**, *6*, A75–A79.
4. Graetz, J.; Ahn, C. C.; Yazami, R.; Fultz, B. Highly Reversible Lithium Storage in Nanostructured Silicon. *Electrochem. Solid-State Lett.* **2003**, *6*, A194–A197.
5. Takamura, T.; Ohara, S.; Uehara, M.; Suzuki, J.; Sekine, K. A Vacuum Deposited Si Film Having a Li Extraction Capacity Over 2000 mAh/g with a Long Cycle Life. *J. Power Sources* **2004**, *129*, 96–100.
6. Obrovac, M. N.; Krause, L. J. Reversible Cycling of Crystalline Silicon Powder. *J. Electrochem. Soc.* **2007**, *154*, A103–A108.
7. Kim, H.; Han, B.; Choo, J.; Cho, J. Three-Dimensional Porous Silicon Particles for Use in High-Performance Lithium Secondary Batteries. *Angew. Chem., Int. Ed.* **2008**, *47*, 1–5.
8. Hochgatterer, N. S.; Schweiger, M. R.; Koller, S.; Raimann, P. R.; Wohrle, T.; Wurm, C.; Winter, M. Silicon/Graphite Composite Electrodes for High-Capacity Anodes: Influence of Binder Chemistry on Cycling Stability. *Electrochem. Solid-State Lett.* **2008**, *11*, A76–A80.
9. Fleischauer, M. D.; Li, J.; Brett, M. J. Columnar Thin Films for Three-Dimensional Microbatteries. *J. Electrochem. Soc.* **2009**, *156*, A33–A36.
10. Chan, C. K.; Peng, H.; Liu, G.; McIlwrath, K.; Zhang, X. F.; Cui, Y. High Performance Lithium Battery Anodes Using Silicon Nanowires. *Nat. Nanotechnol.* **2008**, *3*, 31–35.
11. Wagner, R. S.; Ellis, W. C. Vapor Liquid Solid Mechanism of Single Crystal Growth. *Appl. Phys. Lett.* **1964**, *4*, 89.
12. Morales, A. M.; Lieber, C. M. A Laser Ablation Method for the Synthesis of Crystalline Semiconductor Nanowires. *Science* **1998**, *279*, 208–211.
13. Kim, H.; Cho, J. Superior Lithium Electroactive Mesporous Si@Carbon Core−Shell Nanowires for Lithium Battery Anode Material. *Nano Lett.* **2008**, *8*, 3688–3691.
14. Cui, L.-F.; Yang, Y.; Hsu, C.-M.; Cui, Y. Carbon−Silicon Core−Shell Nanowires as High Capacity Electrode for Lithium Ion Batteries. *Nano Lett.* **2009**, *9*, 3370–3374.
15. Cui, L.-F.; Ruffo, R.; Chan, C. K.; Peng, H.; Cui, Y. Crystalline-Amorphous Core−Shell Silicon Nanowires for High Capacity and High Current Battery Electrodes. *Nano Lett.* **2009**, *9*, 491–495.
16. Park, M.-H.; Kim, M. G.; Joo, J.; Kim, K.; Kim, J.; Ahn, S.; Cui, Y.; Cho, J. Silicon Nanotube Battery Anodes. *Nano. Lett.* **2009**, *9*, 3844–3847.
17. Holmes, J. D.; Johnston, K. P.; Doty, R. C.; Korgel, B. A. Control of Thickness and Orientation of Solution-Grown Silicon Nanowires. *Science* **2000**, *287*, 1471–1473.
18. Hanrath, T.; Korgel, B. A. Supercritical Fluid−Liquid−Solid (SFLS) Synthesis of Si and Ge Nanowires Seeded by Colloidal Metal Nanocrystals. *Adv. Mater.* **2003**, *15*, 437–440.
19. Heitsch, A. T.; Fanfair, D. D.; Tuan, H.-Y.; Korgel, B. A. Solution−Liquid−Solid (SLS) Growth of Silicon Nanowires. *J. Am. Chem. Soc.* **2008**, *130*, 5436–5437.

20. Tuan, H.-Y.; Korgel, B. A. Importance of Solvent-Mediated Phenylsilane Decomposition Kinetics for High-Yield Solution-Phase Silicon Nanowire Synthesis. *Chem. Mater.* **2008**, *20*, 1239–1241.
21. Murugan, A. V.; Muraliganth, T.; Manthiram, A. Comparison of Microwave Assisted Solvothermal and Hydrothermal Synthesis of $LiFePO_4$/C Nanocomposite Cathodes for Lithium Ion Batteries. *J. Phys. Chem. C* **2008**, *112*, 14665–14671.
22. Wilson, A. M.; Dahn, J. R. Lithium Insertion in Carbons Containing Nanodispersed Silicon. *J. Electrochem. Soc.* **1995**, *142*, 326–332.
23. Wang, W.; Datta, M. K.; Kumta, P. N. Silicon-Based Composite Anode for Li-Ion Rechargeable Batteries. *J. Mater. Chem.* **2007**, *17*, 3229–3237.
24. Wang, W.; Kumta, P. N. Reversible High Capacity Nanocomposite Anodes of Si/C/SWNTs for Rechargeable Li-Ion Batteries. *J. Power Sources* **2007**, *172*, 650–658.
25. Wang, G. X.; Ahn, J. H.; Yao, J.; Bewlay, S.; Liu, H. K. Nanostructured Si−C Composite Anodes for Lithium-Ion Batteries. *Electrochem. Commun.* **2004**, *6*, 689–692.
26. Guo, Z. P.; Milin, E.; Wang, J. Z.; Chen, J.; Liu, H. K. Silicon/Disordered Carbon Nanocomposites for Lithium-Ion Battery Anodes. *J. Electrochem. Soc.* **2005**, *152*, A2211–A2216.
27. Ng, S.-H.; Wang, J.; Wexler, D.; Konstantinov, K.; Guo, Z.-P.; Liu, H.-K. Highly Reversible Lithium Storage in Spheroidal Carbon-Coated Silicon Nanocomposites as Anodes for Lithium-Ion Batteries. *Angew. Chem., Int. Ed.* **2006**, *45*, 6896–6899.
28. Zhang, T.; Fu, L.; Gao, J.; Yang, L.; Wu, Y.; Wu, H. Core−Shell Si/C Nanocomposite as Anode Material for Lithium Ion Batteries. *Pure Appl. Chem.* **2006**, *78*, 1889–1896.
29. Chan, C. K.; Ruffo, R.; Hong, S. S.; Huggins, R. A.; Cui, Y. Surface Chemistry and Solid Electrolyte Interphase of Silicon Nanowire Anodes in Lithium-Ion Batteries. *J. Power Sources* **2009**, *189*, 1132–1140.
30. Yen, Y.-C.; Chao, S.-C.; Wu, H.-C.; Wu, N.-L. Study on Solid-Electrolyte-Interphase of Si and C-Coated Si Electrodes in Lithium Cells. *J. Electrochem. Soc.* **2009**, *156*, A95–A102.
31. Che, G.; Lakshmi, B. B.; Fisher, E. R.; Martin, C. R. Carbon Nanotubule Membranes for Electrochemical Energy Storage and Production. *Nature* **1998**, *393*, 346–349.
32. Frackowiak, E.; Gautier, S.; Gaucher, H.; Bonnamy, S.; Beguin, F. Electrochemical Storage of Lithium in Multiwalled Carbon Nanotubes. *Carbon* **1999**, *37*, 61.
33. Gao, B.; Bower, C.; Lorentzen, J. D.; Fleming, L.; Kleinhammes, A.; Tang, X. P.; McNeil, L. E.; Wu, Y.; Zhou, O. Enhanced Saturation Lithium Composition in Ball-Milled Single-Walled Carbon Nanotubes. *Chem. Phys. Lett.* **2000**, *327*, 69.
34. Pushparaj, V. L.; Shaijumon, M. M.; Kumar, A.; Murugesan, S.; Ci, L.; Vajtai, R.; Linhardt, R. J.; Nalamasu, O.; Ajayan, P. M. Flexible Energy Storage Devices Based on Nanocomposite Paper. *Proc. Natl. Acad. Sci. U.S.A.* **2007**, *104*, 13574–13577.
35. Kumar, T. P.; Ramesh, R.; Lin, Y. Y.; Fey, G. T. K. Tin-Filled Carbon Nanotubes as Insertion Anode Materials for Lithium-Ion Batteries. *Electrochem. Commun.* **2004**, *6*, 520.
36. Yoon, S.; Ka, B. H.; Lee, C.; Park, M.; Oh, S. M. Preparation of Nanotube TiO_2-Carbon Composite and Its Anode Performance in Lithium-Ion Batteries. *Electrochem. Solid-State Lett.* **2009**, *12*, A28–A32.
37. Muraliganth, T.; Murugan, A. V.; Manthiram, A. Nanoscale Networking of $LiFePO_4$ Nanorods Synthesized By a Microwave-Solvothermal Route with Carbon Nanotubes for Lithium Ion Batteries. *J. Mater. Chem.* **2008**, *18*, 5661–5668.
38. Lu, X.; Kang, F.; Shen, W. A Comparative Investigation on Multiwalled Carbon Nanotubes and Carbon Black as Conductive Additive. *Electrochem. Solid-State Lett.* **2006**, *9*, A126–A129.
39. Sakamoto, J. S.; Dunn, B. Vanadium Oxide-Carbon Nanotube Composite Electrodes for Use in Secondary Lithium Batteries. *J. Electrochem. Soc.* **2002**, *149*, A26–A30.
40. Ishihara, T.; Nakasu, M.; Yoshio, M.; Nishiguchi, H.; Takita, Y. Carbon Nanotube Coating Silicon Doped with Cr as a High Capacity Anode. *J. Power Sources* **2005**, *146*, 161–165.
41. Kim, T.; Mo, Y. H.; Nahm, K. S.; Oh, S. M. Carbon Nanotubes (CNTs) as a Buffer Layer in Silicon/CNTs Composite Electrodes for Lithium Secondary Batteries. *J. Power Sources* **2006**, *162*, 1275–1281.
42. Shu, J.; Li, H.; Yang, R.; Shi, Y.; Huang, X. Cage-like Carbon Nanotubes/Si Composite as Anode Material for Lithium Ion Batteries. *Electrochem. Commun.* **2006**, *8*, 51–54.
43. Zhang, Y.; Zhao, Z. G.; Zhang, X. G.; Zhang, H.-L.; Li, F.; Liu, C.; Cheng, H.-M. Pyrolytic Carbon-Coated Silicon/Carbon Nanotube Composites: Promising Application for Li-Ion Batteries. *Int. J. Nanomanuf.* **2008**, *2*, 4–15.
44. Chan, C. K.; Ruffo, R.; Hong, S. S.; Huggins, R. A.; Cui, Y. Structural and Electrochemical Study of the Reaction of Lithium with Silicon Nanowires. *J. Power Sources* **2009**, *189*, 34–39.
45. Cui, L.-F.; Ruffo, R.; Chan, C. K.; Peng, H.; Cui, Y. Crystalline-Amorphous Core−Shell Silicon Nanowires for High Capacity and High Current Battery Electrodes. *Nano Lett.* **2009**, *9*, 491–495.
46. Kaempgen, M.; Chan, C. K.; Ma, J.; Cui, Y.; Gruner, G. Printable Thin Film Supercapacitors Using Single-Walled Carbon Nanotubes. *Nano Lett.* **2009**, *9*, 1872–1876.
47. Zhang, Y.; Zhang, X. G.; Zhang, H. L.; Zhao, Z. G.; Li, F.; Liu, C.; Cheng, H. M. Composite Anode Material of Silicon/Graphite/Carbon Nanotubes for Li-Ion Batteries. *Electrochim. Acta* **2006**, *51*, 4994–5000.
48. Wachtler, M.; Wagner, M. R.; Schmied, M.; Winter, M.; Besenhard, J. O. The Effect of the Binder Morphology on the Cycling Stability of Li-Alloy Composite Electrodes. *J. Electroanal. Chem.* **2001**, *510*, 12–19.
49. Li, J.; Lewis, R. B.; Dahn, J. R. Sodium Carboxymethyl Cellulose: A Potential Binder for Si Negative Electrodes for Li-Ion Batteries. *Electrochem. Solid-State Lett.* **2007**, *10*, A17–A20.
50. Thompson, A. H. Electrochemical Potential Spectroscopy: A New Electrochemical Measurement. *J. Electrochem. Soc.* **1979**, *126*, 608–616.